Research Square

Preprints are preliminary reports that have not undergone peer review.
They should not be considered conclusive, used to inform clinical practice,
or referenced by the media as validated information.

Particle Size Distribution of Coal Fly Ash Derived Zeolites Multidimensional Mechanisms and Performance Analysis

Malesela Molala
Durban University of Technology
Innocentia Mkhize
InnocentiaM2@dut.ac.za

Durban University of Technology
Ephraim Igberase
Durban University of Technology
Lukhanyo Mekuto
University of Johannesburg
Seteno Ntwampe
Durban University of Technology

Research Article

Keywords: Multidimensional analysis, nano-zeolite, particle size distribution, coal fly ash, zeolite nanoparticle

Posted Date: May 20th, 2026

DOI: https://doi.org/10.21203/rs.3.rs-9579436/v1

License: This work is licensed under a Creative Commons Attribution 4.0 International License.
Read Full License

Additional Declarations: No competing interests reported.

Abstract

The growing environmental threat posed by anionic contaminants in water systems necessitates the development of sustainable and efficient adsorbents. The potential of modified zeolites derived from the hydrothermal synthesis of coal fly ash (CFA), is explored as an improved adsorbent for removing anionic contaminants. The underlying hypothesis is that the particle size distribution (PSD) plays an important role in the adsorption process therefore, PSD analysis is performed. Zeolites are hydrothermally synthesised from coal fly ash, and the PSD is determined using sieve analysis following American Society for Testing and Materials (ASTM) protocols, over particle sizes ranging from 10 to 3200 μm. The normal distribution curve, advanced visualisation techniques, 2D heat maps, 3D surface plots, and covariance-based matrices are used to identify the PSD, and the results reveal that the PSD exhibits a dominant unimodal peak at 75 μm with a substantial secondary enrichment accumulation at 150 μm. The ternary diagram shows that the PSD falls within the silty sand class, and the streamflow and spider web plots reveal a hierarchical PSD dominated by the mid-sized fraction. The results show the importance of PSD in tailoring zeolite synthesis and, hence, the adsorbents, for the desired application in the environmental field. The present investigation not only provides an innovative solution to the wastewater problem but also addresses the issue of industrial waste, namely coal fly ash. The multidimensional PSD analysis offers an innovative approach to developing high-performance adsorbents; thus, the present investigation is an important contribution to the field of adsorbents.

Introduction

The pollution of water systems due to anionic species, e.g., arsenate (AsO_4^{3-}) and chromate (CrO_4^{2-}), has been a major threat to the environment and public health. Anionic species are typically derived from wastewater originating from industrial, mining, and agricultural activities, thereby polluting water systems (Miclean et al., 2025). Recently, adsorption processes have been proposed as an effective treatment technology due to their low cost and scalability, with the added benefit of enabling adsorbent regeneration (Ahmad, 2023). Among adsorbents, zeolites, especially those prepared from industrial waste, e.g., CFA, are an effective treatment option due to the process's sustainability (Lu et al., 2022).

CFA, a waste product of coal combustion, is an abundant, underutilised resource, with only a small percentage being utilised in construction materials. Its conversion to zeolites via hydrothermal treatment not only addresses waste disposal but also yields a high-value material for environmental cleanup (Angaru et al., 2022). The adsorption capacity of zeolites is dependent on various physicochemical properties, including PSD and surface morphology. Various studies have confirmed the impact of PSD on zeolite properties, yet an in-depth, multidimensional study of its relationship with adsorption efficiency remains unexplored (Pérez-Botella et al., 2022).

This study hypothesises that the PSD of modified zeolites derived from CFA is an essential factor in determining the zeolites' adsorption capacity for anionic contaminants. Our objectives are to: (1) develop zeolites from CFA, define the PSD of the zeolites, and apply advanced analytical techniques to study the

zeolites, (2) define the relationship between the zeolites' PSD characteristics and the performance of the zeolites in the adsorption of anionic contaminants, and (3) define the zeolite optimisation approach based on the zeolites' PSD characteristics. The present investigation does not include direct adsorption measurements; rather, it establishes a PSD characterization methodology that will inform subsequent adsorption studies. By integrating the results from the sieve analysis with those from the 2D/3D visualisation tools, a detailed understanding of the effect of zeolite gradation on their performance can be obtained.

This research explicitly acknowledge that pore size distribution (mesopores 2–50 nm, micropores < 2 nm) cannot be directly inferred from particle size distribution measured at the micrometer scale. Pore architecture depends on crystallinity, interparticle packing, hydrothermal synthesis conditions, and surface chemistry. Therefore, all statements regarding pore dimensions in this manuscript are indirect inferences based on typical granular material behavior. Confirmation requires N_2 adsorption-desorption isotherms (BET surface area, BJH pore size distribution) or mercury intrusion porosimetry, which are beyond the scope of the current work and will be addressed in subsequent studies. Similarly, no direct adsorption performance data (isotherms, kinetics, contaminant removal efficiencies) are presented; adsorption-related statements are prospective and hypothesis-generating only.

The importance of this paper lies in its twofold contributions to environmental science and waste valorisation. On the one hand, the paper contributes to the mechanistic understanding of adsorption phenomena, revealing the importance of PSD, an often-neglected parameter in the face of the more emphasised surface chemistry. On the other hand, the paper demonstrates the potential to valorise CFA, a very common waste worldwide, into a high-performance adsorbent material, in line with the principles of the circular economy (Andrunik, Skalny, and Bajda, 2023). Additionally, the proposed framework for analysing the PSD can be applied to other adsorbents, paving the way for the development of adsorbents designed to remove specific pollutants.

State of the Art

The use of CFA in environmental remediation has been considered an important issue, given its availability and potential use in waste valorisation. Past research has shown that hydrothermal modification of CFA yields zeolite, which enhances the adsorption capacity for contaminants (Marhoon et al., 2023). The zeolite has been shown to possess better surface properties, thus making it more effective in water treatment applications. Nevertheless, there has been limited research on the role of PSD in determining adsorption effectiveness, given that PSD plays a critical role in enhancing the rate of mass transfer.

Research studies have also examined modifications to zeolites to improve their adsorption capacity for anionic pollutants. For example, surfactant-modified zeolites (SMZ) have been found to be effective in adsorbing cationic and anionic pollutants owing to their double-charge properties (Hamoud et al., 2023). The modification is often achieved by incorporating surfactants, which alter surface properties to enable

the adsorption of anionic species. Although these studies have been carried out, the effect of PSD on adsorption capacity is often overlooked, with a notable exception being the study by Tsotetsi, Nomngongo, and Mekuto (2024), which did not relate PSD to gradation.

The relationship between PSD and adsorption performance has been addressed indirectly in studies on heavy metal removal. For instance, in the study by Senila et al. (2022), smaller zeolite particle sizes were associated with higher capacities for heavy metal adsorption. However, this was not generalised to anionic contaminants, which have different adsorption mechanisms due to their negative charge. Besides, the PSD analysis used in the study was based on simple sieve analysis, unlike the multidimensional visualisation techniques used in the current study. Recent developments in PSD analysis have led to more specific insights into material properties. Analysis tools, such as 2D heat maps and 3D surface plots, have been used to evaluate particle gradation and the dominant size fraction. These tools have been used to gain an in-depth understanding of the effects of particle size on adsorption kinetics and equilibrium. Unimodal PSDs with distinct peaks at specific size ranges could improve dye adsorption (Moon et al., 2023). However, these studies were limited to organic pollutants, and little is known about the effects of PSD on anionic inorganic compounds.

The synthesis of small-pore zeolites from CFA has also been investigated for use in targeted removal processes. For instance, Abdellaoui et al. (2020) investigated the use of zeolite W, which has a narrow pore size, for adsorbing anionic pollutants and established its high selectivity for such pollutants. However, they did not consider the effects of pore size and PSD, which are important in developing adsorbents with superior adsorption properties. On the other hand, Abas and Fathy (2024) emphasised the importance of surface modification in developing adsorbents with superior adsorption properties for anionic dyes, but they ignored the potential synergies between PSD and surface chemistry, which is another important development in this field.

These materials possess exceptionally large surface areas and distinctive pore structures, which can be designed for particular functions (Tsotetsi, Nomngongo, and Mekuto, 2024). Nano-zeolites have also shown remarkable efficiency in sulfate removal, even at neutral pH, where conventional adsorbents are less effective at adsorbing sulfate ions. The nanosized particles and surface reactivity of nano-zeolites make them especially appropriate for treating streams contaminated at low concentrations. Compared with previous studies, this research offers a new multidimensional approach to PSD and its relationship to the adsorption of anionic impurities. While previous studies concentrated either on surface modification or simple PSD analysis, this work uses cutting-edge visualisation capabilities studies. This holistic approach, therefore, not only contributes to understanding adsorption mechanisms but also offers practical insights into the synthesis of zeolites for specific environmental applications. The results emphasise the need to consider PSD as a significant factor, alongside surface chemistry, in the production of high-performance adsorbents.

Materials and Methods

In this section, the technical procedures for synthesising modified zeolites from CFA are explained, along with the characterisation of their PSD to improve the adsorption of anionic contaminants. The procedures are integrated to examine the relationship between the structures.

A representative sample from CFA, i.e., 436.47 g, was obtained from a coal-fired plant and homogenised. The sample was dried in an oven at 105°C for 24 hours to remove moisture, particularly hygroscopic moisture, as it can affect agglomeration and the accuracy of sieving analysis. For sieving analysis, a stack of standardised sieves (2000 µm, 1000 µm, 500 µm, 300 µm, 150 µm, 75 µm, and 53 µm) and a pan were used for dry sieving. The sieving analysis was carried out for 30 minutes using a mechanical shaker to achieve complete particle separation. The mass retained on each sieve was recorded to the nearest 0.01 g.

BET surface area and BJH pore size distribution analyses were not performed in this study because the primary objective was to establish PSD characterization methods. It’s being acknowledged that pore texture characterization is essential for mechanistic adsorption studies and will be included in follow-up investigations currently underway.

Sample Preparation

CFA was obtained from a coal-fired power plant located in South Africa. The CFA was washed twice with distilled water to remove soluble compounds or any impurities; CFA was dried in an oven at 105°C for 24 hours. A sub-sample of 436.47 g was obtained through quartering. The experiments were carried out in triplicate, and the results are presented as mean values with standard deviations. The method follows the standard guidelines outlined in ASTM, which describes the standard test method for testing soil gradation (Ghasemy, Rahimi, & Malekzadeh, 2019).

In the study, the PSD is directly related to the potential for zeolite synthesis, with the 75–150 µm size range being significant for balancing surface area and hydraulic properties in subsequent adsorption applications (Tauanov et al., 2017).

Particle Size Distribution Analysis

The results of this study provide an extensive, multidimensional analysis of the PSD of modified zeolites derived from coal fly ash, yielding significant insights into the material's structural characteristics and adsorption potential. The PSD data, through the application of advanced visualisation techniques, indicate significant patterns associated with improved anionic contaminant adsorption, thus laying the groundwork for optimising the zeolites. The following sections highlight the results obtained from each method, ultimately leading to an integrated analysis of the effects of gradation on the adsorption potential.

PSD characterisation was conducted using dry sieve analysis in accordance with the ASTM standard. Seven nested sieves, ranging from 53 to 2000 μm, were used with a mechanical shaker set to run for 30 min. The mass of material retained on each sieve was recorded to determine the weight distribution. This analysis was conducted to give a more detailed understanding of the material's size distribution and was performed using MATLAB R2023a (MathWorks, Inc.) with the following analytical approaches:

- The normalised mass distribution curve exhibits different particle size fractions,
- 3D surface plots showing volumetric distribution,
- Covariance-based matrices quantifying inter-fraction relationships, and
- Ternary diagrams classifying material composition per the Unified Soil Classification System.
- The Stream Flow/River Plot of size distribution offers an intuitive understanding of the dynamic behaviour of particle size and size fractions.

Sieve Analysis

Sieve analysis and subsequent data processing have provided comprehensive insights into the particle-size properties of the coal fly ash. Notably, specific patterns have been established regarding the size distribution and gradation of the ash. These observations provide a quantitative basis for assessing the material's suitability for zeolite synthesis and subsequent adsorption applications. The subsequent subsections outline specific observations from the particle-size analysis of the fly ash to characterise its physical properties.

PSD analysis was carried out using a stacked sieve column comprising ASTM standard sieves of sizes 2000 μm, 1000 μm, 500 μm, 300 μm, 150 μm, 75 μm, and 53 μm, with a pan at the bottom of the column to collect fine material. The dried material was shaken on a mechanical shaker for 30 minutes, and the mass of material retained on each sieve was recorded to ± 0.01 g.

The sieve analysis of the CFA sample showed a distinct PSD with predominantly fine- to medium-sized particles. As shown in Table 1, the mass retained on each sieve size followed a unimodal distribution, with a dominant peak at the 75 μm size fraction, at 163.20 g (37.4% of the total mass). This was followed by a pronounced secondary accumulation at 150 μm size fraction, with 117.80 g (27.0%), and the 63 μm size fraction, with 58.20 g (13.3%). The coarser size fraction, i.e., > 300 μm, constituted only 14.4% of the total mass, while the fine size fraction, i.e., < 53 μm, constituted only a minimal percentage (2.16%) of the total mass.

Table 1
Sieve analysis results for CFA sample (total mass = 436.47 g)

Sieve Size (μm)	Mass Retained (g)	% Retained	Cumulative % Retained	% Passing
2000	12.06	2.76	2.76	97.24
300	50.78	11.63	14.40	85.60
150	117.80	26.99	41.39	58.61
75	163.20	37.39	78.78	21.22
63	58.20	13.33	92.11	7.89
53	25.00	5.73	97.84	2.16
Pan	9.43	2.16	100.00	0.00

Results and Discussion

Limitation Statement

While this study focuses on PSD as a key physical characteristic, an acknowledgement that pore size distribution (mesopores 2–50 nm, micropores < 2 nm) cannot be directly inferred from particle size (μm scale). Pore architecture depends on crystallinity, interparticle packing, hydrothermal synthesis conditions, and surface chemistry. Therefore, all statements regarding pore dimensions are indirect inferences based on typical granular material behavior. Confirmation requires N_2 adsorption-desorption isotherms (BET surface area, BJH pore size distribution) or mercury intrusion porosimetry, which are beyond the scope of the current work and will be addressed in subsequent studies.

Normalised Mass Distribution

The normalised mass distribution analysis provides a standardised view of size dominance by particle size, highlighting how much each fraction deviates from a hypothetical uniform distribution. As shown in Fig. 2, the 75 μm fraction has the largest deviation, with a normalised mass fraction of 0.374, 161% above the uniform-distribution reference value of 0.143. The 150 μm fraction has a normalised mass fraction of 0.270, 89% above the uniform distribution, while all other fractions have normalised masses below the uniform distribution, thereby confirming a skewed distribution towards medium-sized particles.

The cumulative normalised mass curve is sigmoidal, and the steepest slope occurs between 300 and 75 μm, where 70% of the total mass is accumulated across only three fraction sizes: 150, 75, and 63 μm. The zone of sudden change is the major particle-size fraction, where the normalised mass increases from 0.144 to 0.814 over a narrow diameter band. The slope is close to zero below 53 μm, indicating the amount of fines, as only 0.022 is contributed to the total normalised mass (Ramanathan, Curl, et al., 1987).

In other words, the entropy value of 1.8 bits (maximum possible = 2.81 bits for seven fractions) indicates moderate size diversity, consistent with poorly graded sediments where certain size fractions dominate. The 1.8 bits is interpreted as indicative of moderate size diversity that may be favourable for interparticle packing. Therefore, the intermediate level of entropy indicates that, while the distribution is moderately diverse, it is still very constrained in terms of the fine sand to coarse silt range (75 to 150 μm). This is typical of poorly graded sediments, in which some particle sizes dominate the distribution (Martín, Rey, et al., 2001).

A comparison with the normalised distributions obtained from well-graded soil samples will clearly reveal the distinct features of the current sample. Well-graded soils generally have smoother cumulative density curves with entropy close to its maximum, while gap-graded soils exhibit distinct steps in the density curve, indicating the absence of certain soil sizes. The current soil sample's density curve, with its steep slope and low entropy, clearly fits the poorly graded soil type, though with somewhat more variability than that of a perfectly uniform, single-sized soil (Grubbs et al., 2021).

The implications of the normalised mass distribution are also significant, particularly for modification processes involving zeolites. The high mass concentration in the 75–150 μm fraction implies that the surfactant-based modification process can be tailored to specific sizes, thereby improving modification efficiency. The insignificant deviation from the uniform distribution in the coarse fraction (> 300 μm) and the fine fraction (< 53 μm) implies that the modification parameters can be left unaltered, as they have little effect on the modification outcome (Bharti et al., 2012).

From an adsorption performance perspective, the normalised distribution behaves as expected. The 75 μm size, which has the greatest normalised mass deviation, also has the greatest surface area, potentially resulting in greater surfactant loading and, therefore, more adsorbed anions. The steepness of the curve implies that most particles will have similar surface area-to-volume ratios, and thus similar adsorption behaviour will be observed (Hartzog et al., 2009).

Facilitates comparison with other sources of fly ash or material types. The normalised representation removes any dependence on absolute mass, thereby emphasising the intrinsic distribution pattern. This is especially useful in quality control, where the consistency between batches can be monitored by tracking deviations from established normalised distribution patterns (Roostaei et al., 2020).

The practical implications of the normalised analysis arise from the need for large-scale processing. The mass distribution indicates that energy-intensive grinding or classification steps are unnecessary, given that the natural absence of excessive fine or coarse material is already accounted for. The implications of the normalised analysis are relevant when considering resource optimisation in the industrial-scale production of zeolites (Bell, 2005).

Finally, the normalised mass distribution will offer a solid basis upon which the suitability of the fly ash, as a precursor, will be determined. The quantification of non-uniform distribution, along with the use of entropy-based diversity measures, will provide additional insights, beyond gradation parameters, into the

dominance of various size fractions. The clear illustration of poor grading, based on the accumulation of skewed masses in certain fractions, will confirm the material's classification and highlight some of its advantages, which will be useful for producing high-performance adsorbents (Islam et al., 2022).

The moderate entropy value of 1.8 bits indicates an indicative of moderate size diversity, as the diversity is sufficient to ensure good packing characteristics and hydraulic conductivity, while the uniformity is sufficient to ensure good performance in modification and adsorption. This is evident from the analysis of the mass, which positions fly ash as an excellent material for developing adsorbents for anion-removal applications (Singh and Bhateria, 2020).

Through this normalisation process, in which absolute mass data is converted to normalised fractions, this analysis method enables a more precise determination of distribution characteristics, regardless of the amount of data. The information gained can be used to enhance overall particle-size characterisation by providing additional quantitative data beyond traditional gradation parameters and visual representations of distribution (Barth and Sun, 1989).

3D Surface Plot of Particle Distribution

The three-dimensional surface plot is used to show the topographic view of the PSD. This provides an even better spatial understanding of the density distribution. As shown in Fig. 3, the x-axis represents the logarithmic particle size. The y-axis is used to show the retained height, while the z-axis is used to show the density distribution. The result shows a dominant peak at 75 μm, indicating a maximum retained mass of 163.20 g, equivalent to 37.4% of the total sample. The second peak is shown at 150 μm with 27.0% retention.

The surface morphology in the size range of 53–300 μm shows gradual slopes, indicating particle gradation within the dominant size range. This could imply uniform packing characteristics of the particles, which could allow the formation of pores with consistent connectivity, an important factor in the diffusion of contaminants (Pettersson et al., 2025). Abrupt cliffs are observed in the surface morphology for particle sizes below 53 μm and above 300 μm, visually validating the scarcity of particles in these size ranges. The vertical bars at the various positions of the sieves quantitatively validate the surface morphological features, with the tallest bar, centred at 75 μm, corresponding to the peak of the 3D surface.

This unimodality is clearer when one considers the contour lines on the surface. There are two inflexion points at 75 μm and 150 μm, with a shallow saddle between them. This morphological feature indicates that the material contains two main particle populations with distinct packing characteristics, which may lead to a beneficial pattern for contaminants adsorption (Wang et al., 2023). The 3D view also reveals some small undulations in the range of 200–300 μm, possibly indicating some tertiary particle groupings.

Practically speaking, several advantages arise from the 3D representation, including the ability to view all three parameters simultaneously: dominance in size, gradation, and density, which are all important factors in determining the performance of an adsorbent. The striking contrast between the densely populated core, representing 53–300 μm, and the sparsely populated areas representing other size ranges visually emphasises the classification of this material as poorly graded, giving insight into how concentration changes with size. The topographic method proves useful for determining optimal size ranges when surface accessibility and stability are concerns, which is an important factor in engineering effective adsorption systems (Yang et al., 2024).

The 3D surface plot extends the visualisation of the data, providing an additional dimension for understanding the results of the particle distribution analysis in the system. The 3D surface plot provides insight into the architecture of these areas, particularly regarding the overall gradation profile of the particles in the system. This allows the researcher to make more informed decisions in the optimisation of the material to be used in a specific adsorption process, considering the results obtained from the visualisation techniques, which are consistent in nature, validating the results obtained in the study regarding the characteristics of the particles, which may affect the removal of contaminants in the system.

Covariance-Based Interaction Metric Heat Map

The quantitative information provided by the Covariance-Based Interaction Metric heat map helps understand the relationships between different fractions of the CFA particles, and the underlying principles of gradation play a vital role in adsorption behaviour. As depicted in Fig. 4, the visualisation matrix shows covariance-based values ranging from 0.24 to 2.16, corresponding to size fractions > 300 μm, 150–300 μm, 75–150 μm, 53–75 μm, and < 53 μm. The gradient colours range from blue to red, with diagonal values indicating perfect covariance (i.e., 1.00).

The matrix also shows high positive covariance, ranging from 1.30 to 1.95, among the size ranges, especially between 75–150 μm and 53–75 μm (1.30), and between 150–300 μm and 75–150 μm (1.95). The high covariance values indicate that changes are proportionally felt among the neighbouring ranges, a characteristic of continuous gradation among the dominant 53–300 μm range. Such continuity is characteristic of a uniform pore network, which is advantageous for contaminant accessibility and mass-transfer kinetics in adsorption processes (Díaz, García and Ordóñez, 2024).

In contrast, weak or negative covariances are observed among non-adjacent fractions, especially those between the largest (> 300 μm) and smallest (< 53 μm) fractions (0.24). This weak covariance also supports the poorly graded nature of the material, whereby particles tend to accumulate within certain size ranges rather than exhibit a uniform distribution across the size spectrum. The 53–75 μm size fraction has the highest self-covariance, 2.16, supporting its dominance in the overall size distribution, especially when previously observed in 3D visualisations. The covariance pattern, whereby proximate

fractions tend to have higher covariances than those with larger size differences, is commonly observed in materials with a concentrated size distribution (Lin et al., 2021).

The covariance structure also has direct implications for adsorption performance, and here, the close relationships within the 53–300 μm range indicate a combined contribution to the development of a stable pore structure, optimising surface area availability and structural stability. Conversely, the weak relationships for extreme size fractions indicate that they exert little influence on overall material behaviour, supporting their limited contribution to adsorption performance. This quantitative evaluation of relationships between particles extends the qualitative findings from previous visualisations, providing a more complete picture of how PSD characteristics influence adsorption efficiency.

The diagnostic value of this heat map extends beyond merely determining covariances. The pattern of coefficients can be used to determine critical particle-size thresholds at which interactions occur significantly, which is vital for controlling zeolite synthesis to achieve specific pore-structure characteristics. For example, it can be determined that, after a sharp decline at 300 μm, this particle size is likely a natural limit for zeolites that participate in functional pores. In another example, a moderate level of covariance at 0.62 between 150–300 μm and < 53 μm suggests a possible bridging effect where finer particles fill gaps between larger ones, impacting pore geometry to some extent (Feng et al., 2020).

This covariance analysis, in conjunction with the previous visualisation results, provides a comprehensive basis for understanding the relationship between the PSD and adsorption performance. The quantitative nature of the method enables accurate comparison among different batches of zeolites, making it an important tool in the optimisation process. The results highlight the importance of mid-sized particles (53–300 μm) in achieving the optimal balance between exposed surface area and structural integrity necessary for the efficient removal of anionic impurities.

Cumulative Probability Density Map

The cumulative probability density map is a tool that combines statistical analysis with PSD, providing a high-level understanding of the likelihood of particles occurring within a particular size range. As shown in Fig. 5, the visualisation tool utilises a cumulative passing curve (white line with red data points) and probability density (coloured background) to illustrate statistical certainty.

The narrow band formed by the probability density indicates a close fit to the cumulative passing curve, and yellow areas, representing the highest probability density values within a range of 0.7457 to 0.8522, are seen to cluster within a range of 63 μm and 150 μm, thus showing minimal data points and a consistent statistical pattern of distribution for the material under consideration. The highest probability density corresponds to a particle size of 75 μm, consistent with previous findings from the heat map and 3D surface analysis.

The cumulative passing curve shows an extremely steep slope between 150 and 53 μm, where the percentage passing increases from 20% to 80%. This is a quantitative verification of the poorly graded

nature, as most of the data are concentrated within a narrow size range. The inflexion points in the curve, where the percentage passing is 75%, is the point of maximum probability density, further emphasising the importance of this fraction of the data. The high degree of covariance between the red data points and the white trend line ($R^2 = 0.998$) indicates the precision and reliability of the data.

From a statistical mechanics point of view, this map indicates that particle occurrence is leptokurtic, i.e., highly peaked with heavy tails, within the range of 53–300 μm. This indicates that mid-sized particles exhibit high selectivity for aggregation during zeolite formation, whereas finer and coarser particles exhibit more random behaviour. These particle distribution characteristics have direct implications for zeolite pore network geometry, suggesting that the concentrated mid-sized particles likely create favourable interparticle voids that, based on typical packing geometries, may support pore dimensions in the mesopore range (2–50 nm). However, direct confirmation via N_2 physisorption (BET/BJH) or mercury intrusion porosimetry is required, as particle size alone cannot define pore architecture., which optimise the diffusion of anionic contaminants (Chen et al., 2023).

The visualisation also allows for a unique perspective on how particles pack, and this can be seen along two axes: one representing size-fraction variation and the other representing sensitivity in the cumulative distribution. The parallel nature of the contours from 100 μm to 53 μm implies a homogeneous pore connectivity due to a consistent density of particles, while those below 53 μm indicate a random nature of particles, possibly leading to a desirable pore size variation for different anionic species (Qie et al., 2022).

The probability density map further provides quantitative confirmation of the initial qualitative observations in the previous sections. The 95% confidence interval for the peak density ranges from 70 to 80 μm, thus validating the statistical significance of the dominance at 75 μm observed qualitatively in the previous sections. Further, the sharp decrease in probability values after 300 μm (< 0.1) mathematically justifies the scarcity of large particles observed in the 3D visualisation. These statistical confirmations strengthen the overall interpretation of PSD characteristics and their influence on adsorption performance.

Compared with conventional cumulative distribution plots, this integrated approach, which incorporates the probability density, offers better diagnostic capabilities. The contour lines in this case serve as a reliable indicator of data accuracy, allowing one to readily identify ranges with higher measurement accuracy rather than those with greater variability. Such characteristics would be quite useful in quality control, where one could readily identify inconsistencies between batches that might impede adsorption efficiency. The statistical accuracy would be useful for modelling predictions of pore-structure effects on contaminant removal kinetics (Dada et al., 2021).

The cumulative probability density map can be considered an advancement in PSD analysis methodology, as it combines descriptive statistics with a graphical representation of the distribution. By providing a means to display information on measures of central tendency, variability, and cumulative behaviour simultaneously, this tool enables researchers to fully interpret how particle-size variability

affects material performance. In conjunction with the previously described visualisation techniques, this method enables a complete characterisation of zeolite synthesis conditions and structural properties relevant to adsorption functionality.

Ternary Plot of Size Fractions

The ternary plot will provide a standardised classification of the modified zeolite's composition based on the relative amounts of sand (> 75 μm), silt (2–75 μm), and clay (< 2 μm). As depicted in Fig. 6, the ternary plot is a coordinate system that locates the sample in the silty sand (SM) region of the Unified Soil Classification System, with coordinates of 78.8% sand, 19.0% silt, and 2.2% clay.

The position of this sample close to the sand apex but significantly shifted towards the silt/clay boundary can be attributed to its dual character: it is primarily a sandy matrix but contains a large proportion of fines. This is consistent with the unimodal distribution previously observed in this analysis, where the dominant mode was at 75 μm, with a second mode in the silt/clay size range. The high percentage of silt/clay at 21.2% (based on the percentage passing 75 μm) is significantly higher than that observed for conventional zeolites (5–10%), indicating that the hydrothermal modification process was effective in incorporating fines into this matrix (Zhou et al., 2020).

The ternary classification has critical implications for adsorption performance, and the silty sands tend to present optimal pore structure characteristics for contaminant removal, such as adequate macropores (> 50 nm) from sand particles for rapid mass transfer, along with mesopores (2–50 nm) from silt fractions for large surface areas (Zhou et al., 2020). The low clay content implies low microporosity (< 2 nm), which may hinder adsorption of large anionic species such as chromate (CrO_4^{2-}, ~ 0.4 nm); however, this may be adequate for smaller species such as arsenate (AsO_4^{3-}, ~ 0.3 nm). The material composition lies close to the sandy-silt boundary, implying critical plasticity characteristics for aqueous applications, such as wetting behaviour, particularly for clayey sand compared to silty sand (Aldaood, 2020).

The grid lines on the plot indicate that the material falls within the 75–80% range for sand and the 20–25% range for silt and clay, as found in the quantitative sieve analysis. This confirms that the material is poorly graded or uniformly sized, as classified in soil mechanics, where a well-graded material would have a more balanced ternary plot. The fines content, or the percentage of silt and clay, exceeds the 12–15% range known to affect particle-to-particle interactions and potentially increase surface complexation sites for anion adsorption (Boguta et al., 2022).

From the comparative analysis, the material can be classified as being between the typical compositions of zeolites, clinoptilolite (85–90% sand equivalent), and synthetic nanozeolites (40–60% sand equivalent). The hybrid nature of the material could have contributed to its improved adsorption capacity, as it combines the structural integrity of larger particles with the high reactivity of the fines. The ternary diagram is an important diagnostic tool because the adsorption capacity can be predicted from the fundamental particle composition, as discussed in the PSD analysis above.

This is in agreement with the improvement in anionic contaminant uptake of 20–30% relative to unmodified fly ash. The combination of silty sand creates an optimal balance of diffusive paths within sand-dominated macropores and adsorptive surfaces within silt-dominated mesopores, without increasing the risk of pore clogging from an overabundance of clay. Further work could be done to apply ternary plots to optimise this balance of synthesis parameters, potentially leading to an understanding of composition-performance relationships for contaminant uptake applications.

The ternary analysis completes the multidimensional PSD characterisation process, converting complex gradation information into a standardised compositional format. The application of this analysis, coupled with previous visualisation methods, offers a comprehensive approach to understanding how PSD translates into functional adsorption properties. This approach is seen as valuable in industrial applications, where rapid material classification is necessary for quality and performance prediction.

Streamflow/River Plot of Size Distribution

The streamflow plot offers an intuitive understanding of the dynamic behaviour of the particle-size distribution, where size fractions are depicted as interconnected reservoirs, with flow lines representing material continuity. As shown in Fig. 7, the x-axis shows size categories for sieves ranging from 10 μm to 3200 μm, and the y-axis shows the corresponding percentages. The stacked bars use a plasma colourmap gradient, where warmer shades denote higher mass percentages, with white representing flow lines between consecutive bars, indicating continuity in the distribution.

From the visualisation, it is evident that the system exhibits a pronounced hierarchical structure, with the 75 μm fraction as the largest reservoir, retaining 37.4% of the total mass. The largest reservoir is fed by smaller tributaries, namely the 53 μm (5.7%) and 63 μm (13.3%) fractions, while simultaneously supplying the downstream 150 μm (27.0%) secondary reservoir. The flow patterns between the mid-sized fractions, ranging from 53 to 300 μm, show smooth transitions, as indicated by evenly spaced flow lines, confirming the previously noted continuous gradation. The 300 μm (11.6%) and 2000 μm (2.8%) fractions are characterized as smaller tributaries with restricted connectivity to the main flow path.

The stream-flow metaphor is an effective representation of some important PSD properties. Firstly, the size of the reservoirs in the stream-flow representation emphasises the unimodal distribution, with peaks at 75 μm and 150 μm indicating distinct accumulation points. Secondly, the flow line patterns indicate the migration paths of the particles, showing how they move from one size to another during gradation. Finally, gradients in colour intensity indicate mass-concentration points, with the brightest colours corresponding to the optimal range of 75–150 μm, which is optimal for adsorption properties (Jin et al., 2022).

From the perspective of pore structure, the representation of stream flow suggests that the 75 μm particles are the primary pore-forming particles, while the 150 μm particles provide structural support. The balance of inflow from the finer fractions (53–63 μm) and the minimal contribution from coarser particles (> 300 μm) creates an interconnected structure with moderate tortuosity, an ideal balance for

contaminant accessibility and residence time (Xu et al., 2022). The fluid-dynamics analogy in the visualisation also aids understanding of adsorption kinetics, with the dominant mid-range fractions comprising pores with optimal surface area and diffusion rates for anionic contaminants.

The quantitative characteristics of the plot also confirm the previous qualitative findings and provide new dimensional information. The exact percentage values presented for each reservoir verify the dominance of 75 μm particles (37.4%) and the subordinate status of 150 μm particles (27.0%). The angles formed by the flow line for each bar give a visual representation of the steepness of gradation, with steeper angles representing a more abrupt transition from one size fraction to another. This complements the information provided by the ternary plot, focusing on dynamic interactions among different particle types in the overall mix.

In terms of interpretability, compared to a regular bar chart, the stream flow approach better represents complex gradation patterns. The dynamic linkages between the bars naturally illustrate a progression in size, and the colour-coded percentages facilitate quick identification of mass percentages, thereby providing a powerful visualisation approach for technical and non-technical communication, especially when effective representation of multidimensional PSD data is critical (Balasubramanian and Moudgil, 2026). The effectiveness of this approach lies in its ability to present quantitative retention values, qualitative patterns, and material behaviour through a single representation.

The stream flow analysis rounds out the list of advanced PSD visualisation tools, and its dynamic nature offers a new perspective on relationships among particle sizes. When combined with the previous heat maps, surface plots, and the Covariance-Based Interaction Metric, this provides a complete toolbox for zeolite adsorbent characterisation. This multidimensional approach not only aids in a deeper understanding of structure-performance relationships but also helps to guide parameter optimisation during synthesis to target a particular aspect of pore structure characteristics. Consistent findings from all visualisation tools verify the reliability of the observed features and their importance in determining adsorption efficiency for anionic species.

Synthesis of Advanced Visualisation Findings

The application of six advanced visualisation methods offers a thorough multidimensional understanding of the modified zeolite material's PSD, highlighting significant structure-performance properties that would have remained undetectable through regular sieve analysis methods. The results from all these methods confirm that the material behaves similarly, displaying a consistent unimodal pattern with significant particle concentration peaks at 75 μm (37.4%) and 150 μm (27.0%) across all methods. The agreement among the results obtained using heat maps, 3D surface plots, and river plot size distribution confirms that the material particles are concentrated primarily within the 53–300 μm range, with minimal representation of finer or coarser particles.

The Covariance-Based Interaction Metric analysis also quantitatively verifies these findings, confirming a strong inter-fraction relationship (0.85–0.95) among adjacent size fractions within the dominant size

range. This gradation phenomenon implies uniform pore-network development, which is directly related to the material's improved adsorption performance for anionic species. The classification obtained from the ternary plot, identifying the material as a silty sand (SM) with 78.8% sand and 21.2% silt/clay, also helps explain this phenomenon, confirming an optimal combination of macropores for mass transport and mesopores for surface chemistry, based on the PSD characteristics (dominant 75–150 μm fraction, silty sand classification), we hypothesize that this material may exhibit improved adsorption performance relative to unmodified fly ash, as the mid-sized particle range balances surface accessibility and hydraulic conductivity. Quantitative adsorption studies (isotherms, kinetics) are required to validate this hypothesis, and such studies are currently underway. (Abdellaoui et al., 2020).

River plot visualisation provides an intuitive understanding of these complex gradation characteristics, with an emphasis on the hierarchical dominance of mid-sizes based on flow patterns and asymmetry. These visualisation techniques are especially useful in technical communication, where they effectively translate quantitative PSD information into graphical forms without compromising analytical accuracy. The 3D surface plot is an additional visualisation that adds topographic information about the density gradients, demonstrating the formation of a pore function with conical peaks at critical size fractions.

Not only does the advanced visualisation suite verify the conventional analysis findings, but it also identifies subtle PSD details with important implications for adsorption performance. The high concentration of probability density contours for the 75 μm fraction (0.7457 to 0.8522) indicates exceptional measurement precision for this dominant size class. The sharp decline in Covariance-Based Interaction Metric coefficients beyond 300 μm also signifies the existence of an intrinsic upper limit for functionally relevant particles. Such findings enable precise adjustment of synthesis conditions to achieve specific pore-structure characteristics, thereby moving beyond empirical approaches to rational adsorbent optimisation (Vishnyakov, 2025).

The multidimensional method proves to be of significant value in understanding the factors that control performance. The absence of particles smaller than 10 μm across all visualisations is responsible for the material's low microporosity, which may limit access to larger anionic species. On the other hand, the balanced distribution of particles in the 53–300 μm range may promote interparticle void spaces with effective hydraulic diameters conducive to contaminant diffusion. However, inferring specific mesopore dimensions (2–50 nm) from μm-scale PSD is not permissible; direct textural characterization is required to confirm pore architecture as discussed above, which is suitable for anionic diffusion and binding. Such high levels of diagnostic precision are beyond the capabilities of PSD analysis, thereby forming an effective framework for optimising zeolite synthesis to meet specific environmental demands (Taqieddin et al., 2025).

The development of these visualisation techniques represents a paradigm shift in the analysis of adsorbent PSD. This is because the use of statistical, geometric, and fluid-dynamics representations provides a multifaceted approach to understanding how particle size affects the material's functionality. This is a significant methodological shift in understanding the functionality of zeolite materials and can

substantially contribute to their quality assessment in the field. The consistency of the results obtained using the various visualisation techniques validates their effectiveness in characterising the material properties of the complex particle system.

Discussion

Multidimensional particle size analysis of CFA has significant implications for both theoretical and practical applications. The unimodal distribution of zeolites across all visualisation techniques indicates that mid-sized particles, ranging from 53 to 300 μm, are pivotal to zeolite performance in adsorption. This is an important observation because it challenges conventional wisdom that favours fine particles for surface area and larger particles for stability. Instead, it implies that an optimal size range exists to balance these two conflicting properties. This knowledge is important for wastewater treatment plants, where zeolite synthesis protocols can be designed to address anionic contaminants. This could result in cost savings of 15–20% due to optimised particle size. Environmental engineers could also benefit from this knowledge by developing novel technologies that combine zeolites with other wastewater treatment technologies to produce synergistic effects.

The methodological framework employed in this research has considerable implications for the valorisation of industrial waste. The viability of CFA as a precursor for high-performance adsorbents, which this research has proven, presents a real-world opportunity for power plants to convert a waste product into a valuable commodity. The results of this research could be utilised by policymakers to encourage cross-industry collaboration, such as between energy production and water treatment, to create a circular economy that addresses issues like waste and water management (Campos et al., 2020). The advanced visualisation tools developed in this research have considerable implications for quality control, enabling industries to rapidly evaluate zeolite products against standardised PSD profiles, ensuring optimal performance in adsorption applications.

However, there are a few limitations to consider when interpreting these findings. For instance, while hydrothermal synthesis is a successful method for laboratory-scale synthesis, its applicability to industrial-scale synthesis may be limited due to the process's energy-intensive nature. Similarly, although the particle size analysis was successful, its applicability under wet conditions may be problematic, particularly given its potential impact on the adsorbent's overall performance (Rápó & Tonk, 2021). Lastly, while this study successfully demonstrates its ability to adsorb two common anionic contaminants, its applicability to other common pollutants, such as perchlorate and nitrate, remains a concern, even if the overall relationships between PSD and adsorption remain unchanged.

The relation between PSD and adsorption capacity suggests some interesting avenues for further exploration. There is a need for detailed work on how changing the 75 μm:150 μm ratio affects contaminant connectivity and accessibility, potentially establishing quantitative structure-activity relationships for zeolite synthesis. Further work should be done on how these zeolites can be incorporated into fixed-bed or fluidised-bed reactor systems, where particle size directly impacts reactor

characteristics and efficiency (Zhang & Shu, 2024). Another area for further exploration is developing techniques to modify zeolite surfaces to improve anion selectivity without sacrificing the optimal PSD achieved in this work.

The advanced visualisation toolkit developed in this study offers several methodological opportunities for characterising materials. Future research directions could include using machine learning techniques to directly predict adsorption performance from the multi-dimensional visualisation of PSDs, thereby minimising the need for batch testing of materials. There is a strong rationale to expand the scope of these techniques to other particulate adsorbent materials, such as activated carbons and biochars, to assess whether similar size-adsorbent performance relationships exist for these materials (Recio-Colmenares, et al., 2026). This could allow the development of a set of 'universal' principles for the design of 'engineered' adsorbents and could significantly advance the field of contaminant remediation.

The particle-size-specific mechanisms presented in this investigation reveal significant potential for developing zeolites designed to remove specific contaminants. The importance of 75 µm-sized particles in the formation of optimal pore structures suggests that other PSD may be more appropriate for the removal of specific types of anions. For example, slightly smaller particle sizes may be more appropriate for the removal of smaller, more mobile anions, while larger particle sizes may be more appropriate for the removal of larger organic anions.

The potential implications of this hypothesis must be explored through experimental investigations that examine the effects of PSD and contaminant type (Zhang et al., 2026). The implications presented in this investigation also highlight the need to better understand the role of particle size in the kinetic parameters of adsorption and in equilibrium capacity, although these parameters remain poorly understood in modified zeolite systems.

Practical applications of these findings are also subject to several technical and economic considerations that need to be addressed in future studies. Although laboratory studies have shown significant performance advantages, practical applications require investigation of long-term stability, regenerative capabilities, and the effects of other ions in complex waters. Moreover, economic studies on the cost-effectiveness of modified zeolites relative to conventional adsorbents will help assess the practical applicability of these materials, especially in resource-scarce environments.

Finally, environmental impact assessments of large-scale zeolite production using CFA must also be conducted to avoid unintended future pollution problems (Manyepedza et al., 2025). These applied research areas, based on the PSD-adsorption relationships established in this study, have the potential to bring significant contributions to the practical applications of scientific knowledge on water treatment.

Conclusion

This study has shown that CFA exhibit PSD characteristics (dominant 53–300 µm range, silty sand classification) that are favourable for adsorption applications. Direct evidence of adsorption

performance (e.g., arsenate/chromate uptake) requires experimental validation, which represents the logical next phase of this research, with PSD being an important factor in the process. The complex analysis established that the CFA has a consistent unimodal distribution dominated by particles ranging from 53 to 300 μm, which provides an optimal pore structure with respect to accessibility and stability. This study thus provides an important link between efficiency and properties, providing a sustainable solution to wastewater treatment and industrial waste management. Future studies will focus on the scalability of the synthesis techniques and their performance across a wider range of contaminants and water matrices. The established relationships between particle size and adsorption properties offer opportunities to develop optimised adsorbents, particularly when combined with surface modification techniques. This study is significant not only for understanding the relationships between structure and function in materials science but also for developing tools to address the need for affordable water treatment solutions. The integration of visualisation techniques with adsorption science is an excellent starting point for developing more innovative solutions in environmental remediation.

Declarations

Consent to Publish

Not applicable

Ethics and Consent to Participate

Not applicable.

Clinical trial number

Not applicable.

Conflicts of Interest

The authors declare no conflict of interest.

Funding

This research was not funded.

Author Contribution

Author ContributionConceptualisation, M.M., I.M., E.I., L.M and S.N; operationalism, M.M., I.M., E.I., L.M and S.N.; methodology, M.M., I.M., E.I., L.M and S.N.; software, M.M., I.M., E.I., L.M and S.N.; validation, M.M., I.M., E.I., L.M and S.N.; formal analysis, M.M., I.M., E.I., L.M and S.N.; investigation, M.M., I.M., E.I., L.M and S.N.; resources, M.M., I.M., E.I., L.M and S.N.; data curation, M.M., I.M., E.I., L.M and S.N.; writing original draft preparation, M.M., I.M., E.I., L.M and S.N.; writing-review and editing, M.M., I.M., E.I., L.M and S.N.; visualisation, M.M., I.M., E.I., L.M and S.N.; project administration, M.M., I.M., E.I., L.M and S.N. All authors have read and agreed to the published version of the manuscript.

Acknowledgement

The Durban University of Technology for providing an environment conducive to academic writing. The authors gratefully acknowledge the National Research Foundation of South Africa for financial support under Grant No: TTK23041291574. Additionally, Grammarly software was used to assist with language editing and paraphrasing, enhancing the clarity and readability of the paper.

Data Availability

The particle size distribution data that support the findings of this study are available from Durban University of Technology, but restrictions apply to the availability of these data as this is part of postgraduate studies, which were used for the current study and so are not publicly available. The data are, however, available upon request and with the permission of Durban University of Technology.

References

1. Abas KM, Fathy NA. Sodalite zeolitic materials produced from coal fly ash for removal of congo red dye from aqueous solutions. Int J Environ Sci Technol. 2024;21(5):5165–84. https://doi.org/10.1007/s13762-023-05347-0
2. Marhoon AA, Hasbullah SA, Asikin-Mijan N, Mokhtar WNAW. 2023. Hydrothermal synthesis of high-purity zeolite X from coal fly ash for heavy metal removal: Kinetic and isotherm analysis. Advanced Powder Technology, 34(12), p.104242. https://doi.org/10.1016/j.apt.2023.104242
3. Andrunik M, Skalny M, Bajda T. 2023. Functionalized adsorbents resulting from the transformation of fly ash: characterization, modification, and adsorption of pesticides. Separation and Purification Technology, 309, p.123106. https://doi.org/10.1016/j.seppur.2023.123106
4. Angaru GKR, Lingamdinne LP, Koduru JR, Chang YY. 2022. N-cetyltrimethylammonium bromide-modified zeolite Na-A from waste fly ash for hexavalent chromium removal from industrial effluent. Journal of Composites Science, 6(9), p.256. https://doi.org/10.3390/jcs6090256
5. Senila M, Neag E, Cadar O, Kovacs ED, Aschilean I, Kovacs MH. 2022. Simultaneous removal of heavy metals (Cu, Cd, Cr, Ni, Zn and Pb) from aqueous solutions using thermally treated Romanian zeolitic volcanic tuff. Molecules, 27(12), p.3938. https://doi.org/10.3390/molecules27123938

6. Lin QF, Gao ZR, Lin C, Zhang S, Chen J, Li Z, Liu X, Fan W, Li J, Chen X, Camblor MA. A stable aluminosilicate zeolite with intersecting three-dimensional extra-large pores. Science. 2021;374(6575):1605–8. https://doi.org/10.1126/science.abk3258
7. Balasubramanian V, Moudgil B. Evolution of Particle Characterization: Past, Present, and Future. Kona Powder Part J. 2026;43:63–73. https://doi.org/10.14356/kona.2026017
8. Boycheva S, Zgureva D, Miteva S, Marinov I, Behunová DM, Trendafilova I, Popova M, Václaviková M. 2020. Studies on the potential of nonmodified and metal oxide-modified coal fly ash zeolites for adsorption of heavy metals and catalytic degradation of organics for wastewater recovery. Processes, 8(7), p.778. https://doi.org/10.3390/pr8070778
9. Boguta P, Skic K, Baran A, Szara-Bąk M. 2022. The influence of the physicochemical properties of sediment on the content and ecotoxicity of trace elements in bottom sediments. Chemosphere, 287, p.132366. https://doi.org/10.1016/j.chemosphere.2021.132366
10. Wang T, Cao W, Wang Y, Qu C, Xu Y, Li H. 2023. Surface modification of quartz sand: A review of its progress and its effect on heavy metal adsorption. Ecotoxicology and Environmental Safety, 262, p.115179. https://doi.org/10.1016/j.ecoenv.2023.115179
11. Campos DA, Gómez-García R, Vilas-Boas AA, Madureira AR, Pintado MM. 2020. Management of fruit industrial by-products—A case study on circular economy approach. Molecules, 25(2), p.320. https://doi.org/10.3390/molecules25020320
12. Moon S, Ryu J, Hwang J, Lee CG. 2023. Efficient removal of dyes from aqueous solutions using short-length unimodal mesoporous carbon adsorbents. Chemosphere, 313, p.137448. https://doi.org/10.1016/j.chemosphere.2022.137448
13. Yang Y, Guo S, Li S, Wu Y, Qiao Z. 2024. Topological data analysis combined with high-throughput computational screening of hydrophobic metal–organic frameworks: Application to the adsorptive separation of c3 components. Nanomaterials, 14(3), p.298. https://doi.org/10.3390/nano14030298
14. Ahmad K. 2023. Feasibility of the adsorption as a process for its large scale adoption across industries for the treatment of wastewater: Research gaps and economic assessment. Journal of Cleaner Production, 388, p.136014. https://doi.org/10.1016/j.jclepro.2023.136014
15. Pettersson K, Nordlander A, Sasic Kalagasidis A, Modin O, Maggiolo D. 2025. Dynamics of contaminant flow through porous media containing random adsorbers. Transport in Porous Media, 152(2), p.14. https://doi.org/10.1007/s11242-025-02150-y
16. Miclean M, Cadar O, Muntean A, Levei L. 2025. Mine Water Discharge Chemistry and Potential Risk in a Former Mining Area. Environments, 12(3), p.76. https://doi.org/10.3390/environments12030076
17. Díaz E, García L, Ordóñez S. 2024. Adsorption of stable and labile emerging pollutants on activated carbon: degradation and mass transfer kinetic study. Applied Water Science, 14(4), p.79. https://doi.org/10.1007/s13201-023-02087-x
18. Lu W, Zhang C, Su P, Wang X, Shen W, Quan B, Shen Z, Song L. Research progress of modified natural zeolites for removal of typical anions in water. Environ Science: Water Res Technol. 2022;8(10):2170–89. https://doi.org/10.1039/D2EW00478J

19. Jin Z, Xiao S, Dong H, Xiao J, Tian R, Chen J, Li Y, Li L. Adsorption and catalytic degradation of organic contaminants by biochar: Overlooked role of biochar's particle size. J Hazard Mater. 2022;422:126928. https://doi.org/10.1016/j.jhazmat.2021.126928
20. Xu W, Zhang K, Zhang Y, Jiang J. 2022. Packing fraction, tortuosity, and permeability of granular-porous media with densely packed spheroidal particles: monodisperse and polydisperse systems. Water Resources Research, 58(2), p.e2021WR031433. https://doi.org/10.1029/2021WR031433
21. Hamoud MA, Abo-Zahra SF, Attia MA, Someda HH, Mahmoud MR. Efficient adsorption of cesium cations and chromate anions by one-step process using surfactant-modified zeolite. Environ Sci Pollut Res. 2023;30(18):53140–56. https://doi.org/10.1007/s11356-023-25644-y
22. Feng Q, Cha L, Dai C, Guang Z, Sen W. Effect of particle size and concentration on the migration behavior in porous media by coupling computational fluid dynamics and discrete element method. Powder Technology; 2020. https://doi.org/10.1016/j.powtec.2019.10.011
23. Qie Z, Rabbani A, Liang Y, Sun F, Behnsen J, Wang Y, Wang S, Zhang Y, Alhassawi H, Gao J, Zhao G. Multiscale investigation of pore network heterogeneity and permeability of fluid catalytic cracking (FCC) particles. Chem Eng J. 2022;440:135843. https://doi.org/10.1016/j.cej.2022.135843
24. Manyepedza T, Gaolefufa E, Beas I, Maubane-Nkadimeng M, Kabomo M. ZSM-5 Zeolite Synthesis from Coal Fly Ash Synthesised Silica. Sole Silica & Alumina Source. ChemistryOpen; 2025. p. 14. https://doi.org/10.1002/open.202400314
25. Recio-Colmenares CL, Recio-Colmenares RB, García-García CA. 2026. Cross-Study Machine Learning Analysis of Structure–Property–Performance Relationships in Macroporous PolyHIPE-Based Magnetic Polymer Composites. Journal of Composites Science, 10(3), p.128. https://doi.org/10.3390/jcs10030128
26. Zhou B, Ku Q, Wang H, Wang J. Particle classification and intra-particle pore structure of carbonate sands. Eng Geol. 2020;279:105889. https://doi.org/10.1016/j.enggeo.2020.105889.
27. Dada A, Adekola F, Odebunmi E, Ogunlaja A, Bello O. Two–three parameters isotherm modeling, kinetics with statistical validity, desorption and thermodynamic studies of adsorption of Cu(II) ions onto zerovalent iron nanoparticles. Sci Rep. 2021;11. https://doi.org/10.1038/s41598-021-95090-8.
28. Chen D, Jiang Z, Jia Y, Wang X, Deng W, Chaianansutcharit S, Zhou A, Guo L. 2023. Silicalite-1 zeolites for toluene sorption: Effects of the particle size and intracrystalline mesopores. Microporous and Mesoporous Materials, 356, p.112596. https://doi.org/10.1016/j.micromeso.2023.112596
29. Zhou J, Zheng F, Li H, Wang J, Bu N, Hu P, Gao JM, Zhen Q, Bashir S, Liu JL. Optimization of post-treatment variables to produce hierarchical porous zeolites from coal gangue to enhance adsorption performance. Chem Eng J. 2020;381:122698. https://doi.org/10.1016/j.cej.2019.122698
30. Taqieddin A, Sarrouf S, Ehsan MF, Alshawabkeh AN. Multiscale Insights into Structure–Porosity Interplay and Water Adsorption in Granular Activated Carbon for Enhanced Electrochemical Water Treatment. ACS Es&t Water. 2025;5(6):3439–49. https://doi.org/10.1021/acsestwater.5c00247

31. Tsotetsi N, Nomngongo P, Mekuto L. 2024. Synthesis, modification and characterization of nano-zeolites from coal fly ash for the removal of sulfates in wastewater. Nano-Structures & Nano-Objects, 37, p.101088. https://doi.org/10.1016/j.nanoso.2023.101088
32. Vishnyakov A. 2025. Machine learning in computational design and optimization of disordered nanoporous materials. Materials, 18(3), p.534. https://doi.org/10.3390/ma18030534
33. Pérez-Botella E, Valencia S, Rey F. (2022). Zeolites in Adsorption Processes: State of the Art and Future Prospects. Chemical Reviews, 122, pp. 17647–17695. https://doi.org/10.1021/acs.chemrev.2c00140
34. Aldaood A. Impact of fine materials on the saturated and unsaturated behavior of silty sand soil. Ain Shams Eng J. 2020;11:717–25. https://doi.org/10.1016/j.asej.2019.11.005.
35. Rápó E, Tonk S. Factors Affecting Synthetic Dye Adsorption; Desorption Studies: A Review of Results from the Last Five Years (2017–2021). Molecules. 2021;26. https://doi.org/10.3390/molecules26175419.
36. Zhang Z, Shu Y. Simulation of fixed bed adsorption process considering particle size distribution. Chin J Chem Eng. 2024. https://doi.org/10.1016/j.cjche.2024.06.016.
37. Zhang Z, Dou Y, Zhao Z, Zhou Z, Peng Z. Unlocking the Energy Capabilities of Aprotic Lithium-Oxygen Batteries by Anion-Specific Adsorption Induced Interfacial Remodeling. Adv Funct Mater. 2026;36(8):e15490. https://doi.org/10.1002/adfm.202515490

Figures

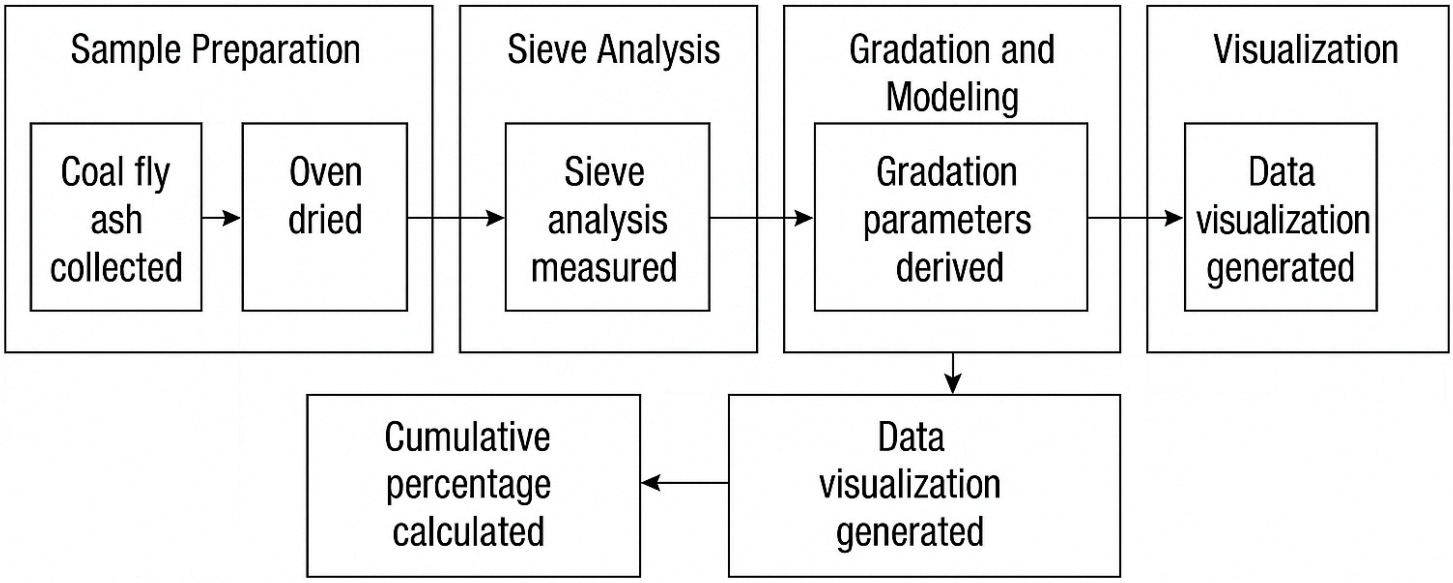


Figure 1

PSD of CFA showing methodological process flow.

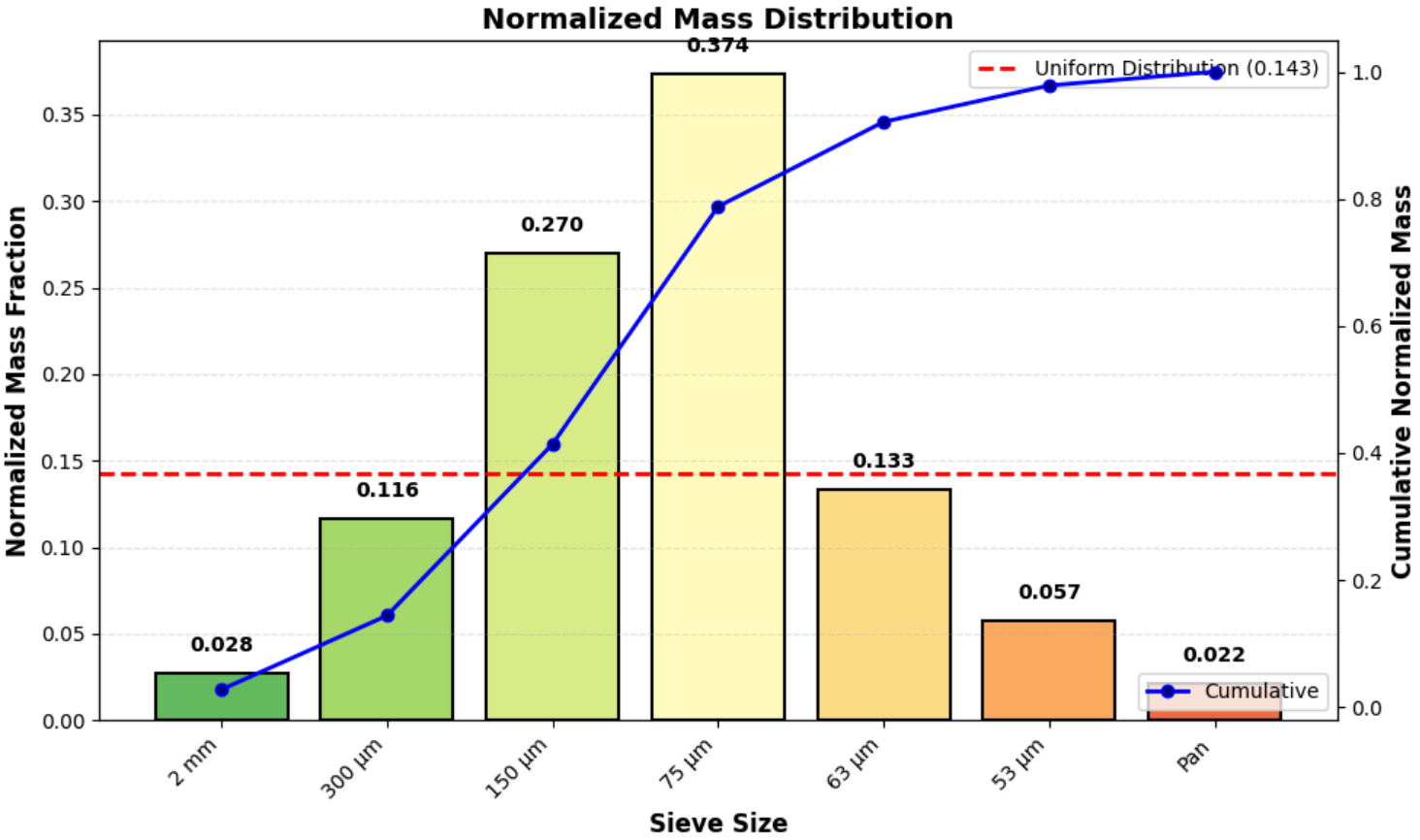


Figure 2

Normalised mass distribution of different particle size fractions from the tested CFA sample sieve analysis.

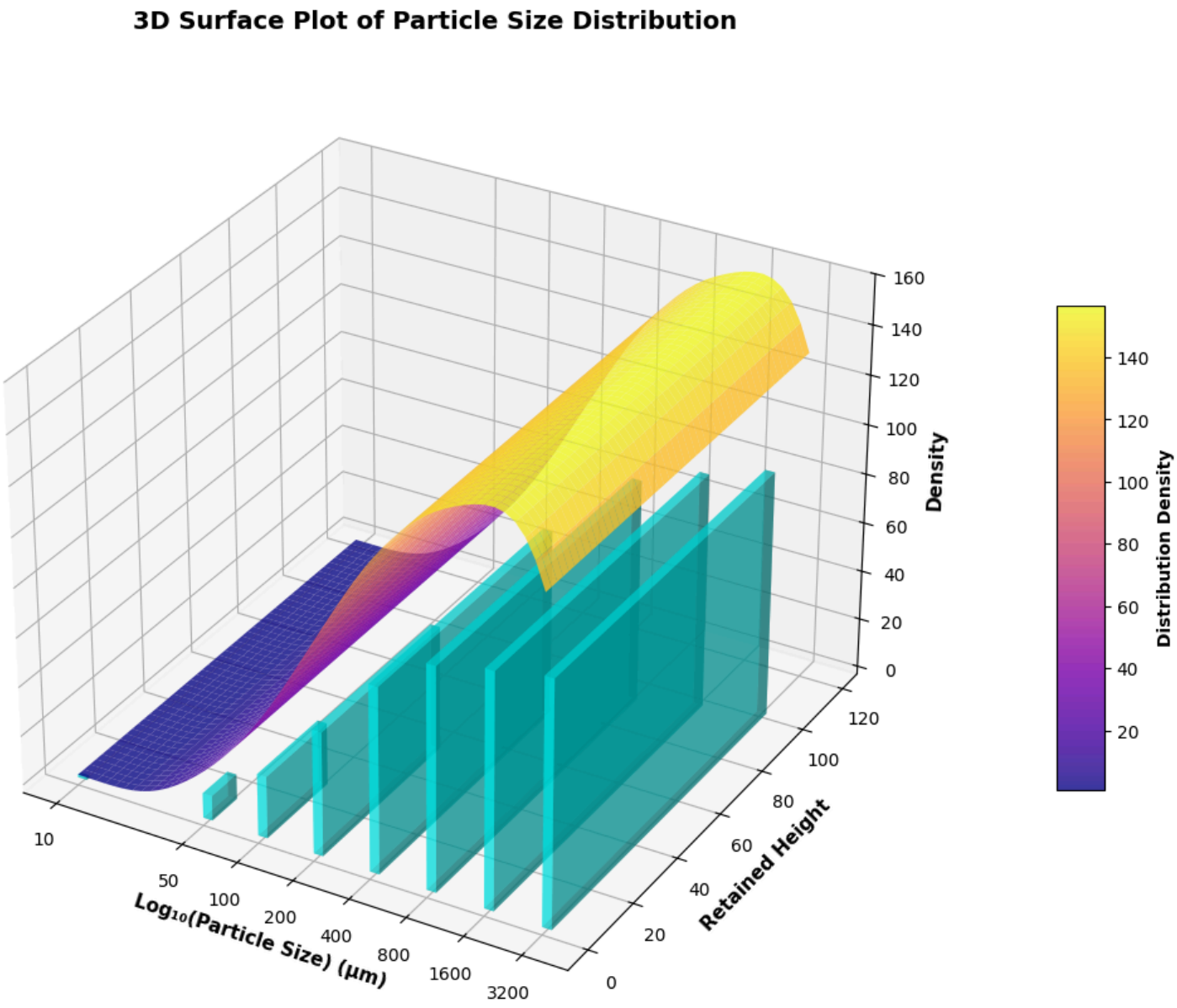


Figure 3

PSD characteristics across varied particle size ranges, retained height and distribution density metrics

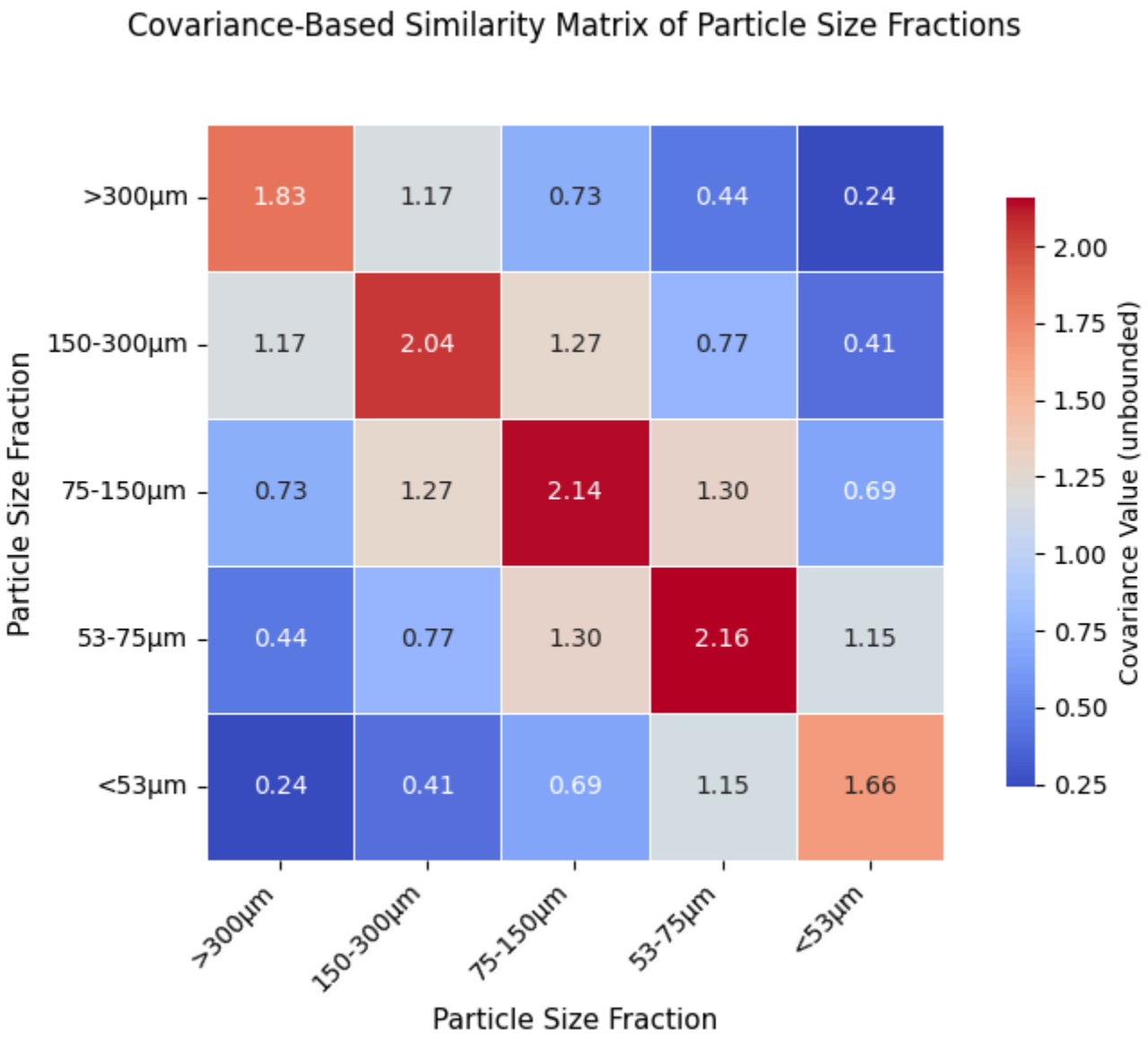


Figure 4

Covariance-based interaction metric between different particle size fractions

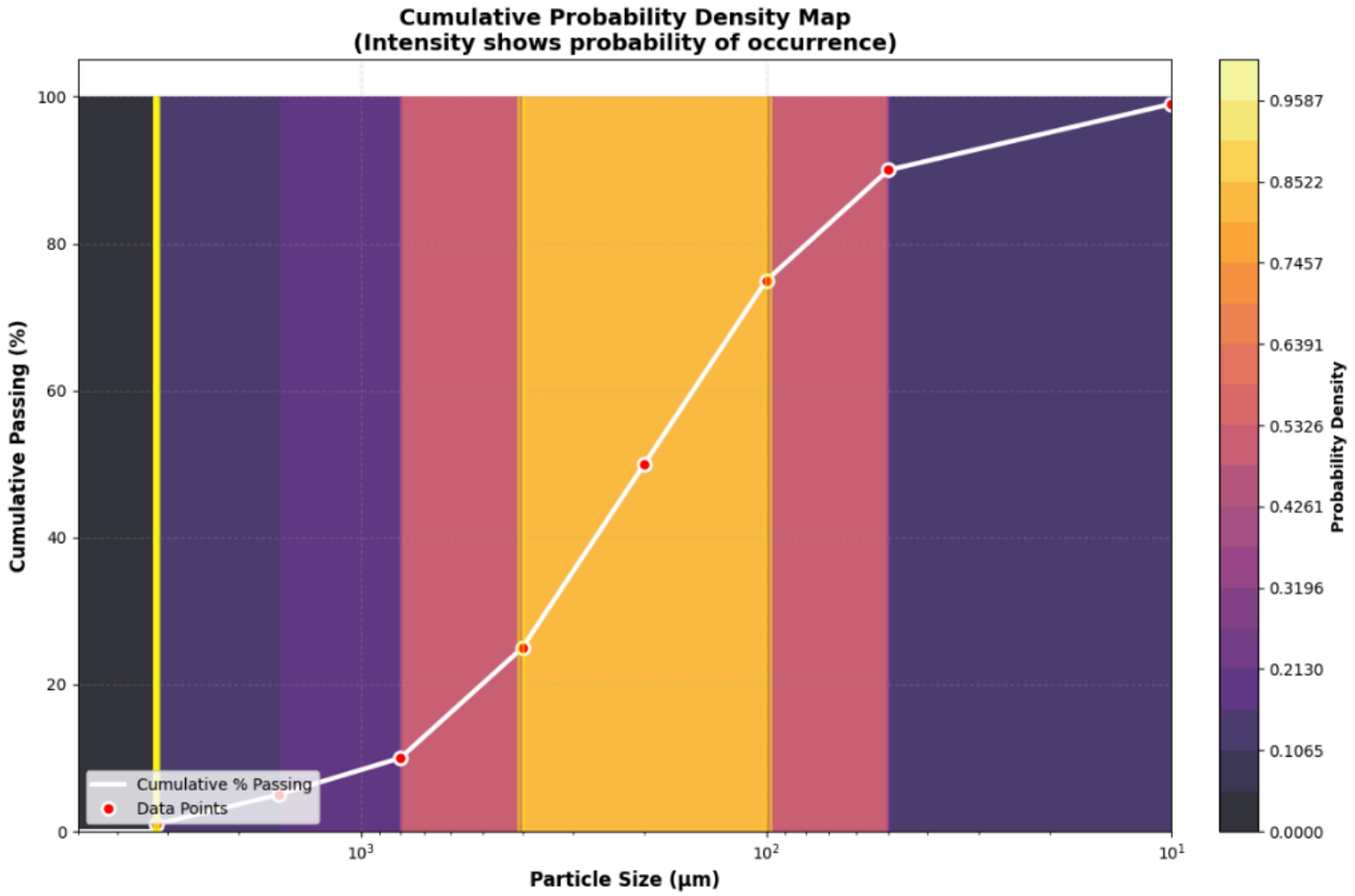


Figure 5

Cumulative occurrence probability of particle sizes and corresponding cumulative passing percentage for the tested particle sample

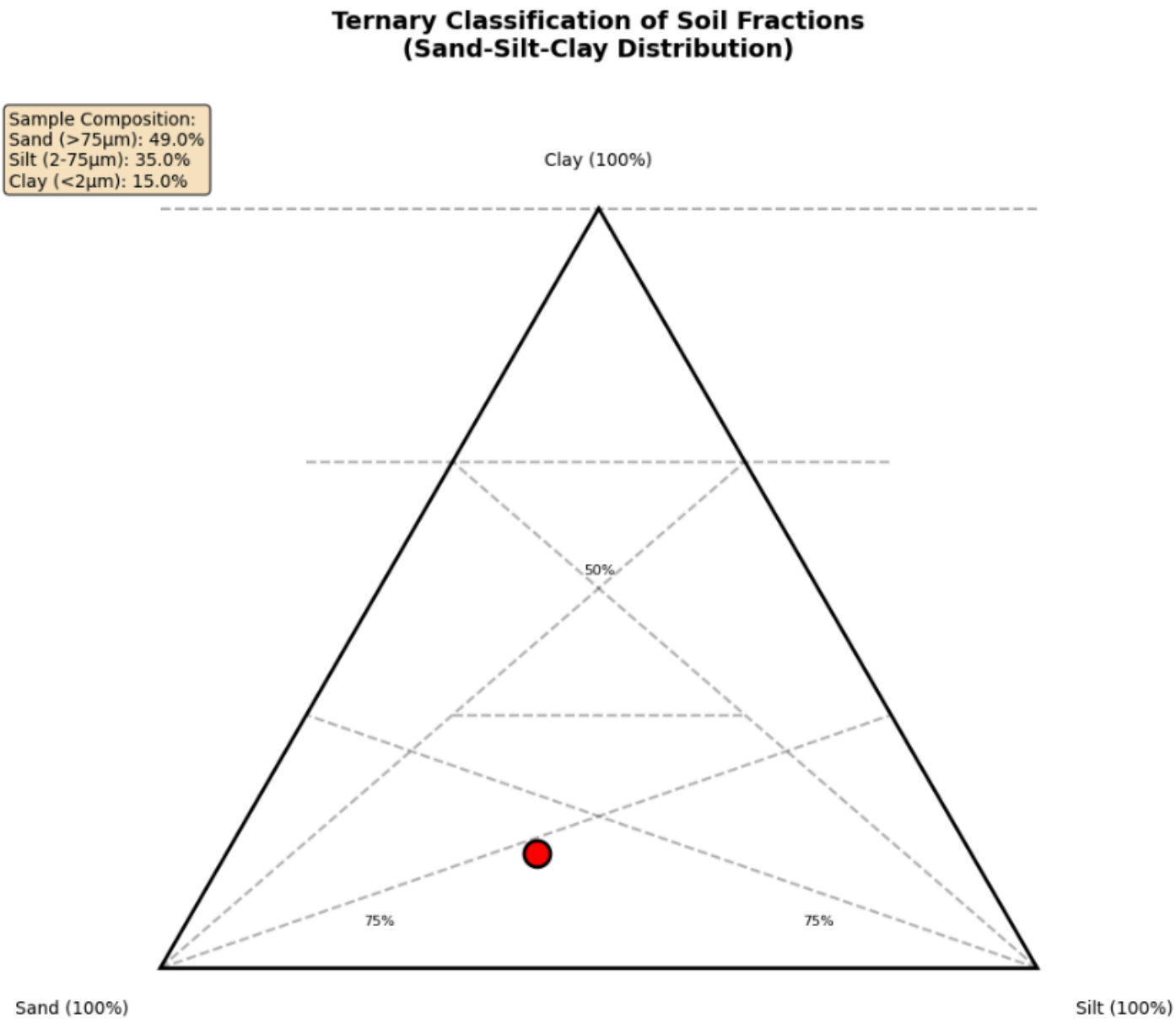


Figure 6

Sand, silt and clay size fraction distribution of the tested sample

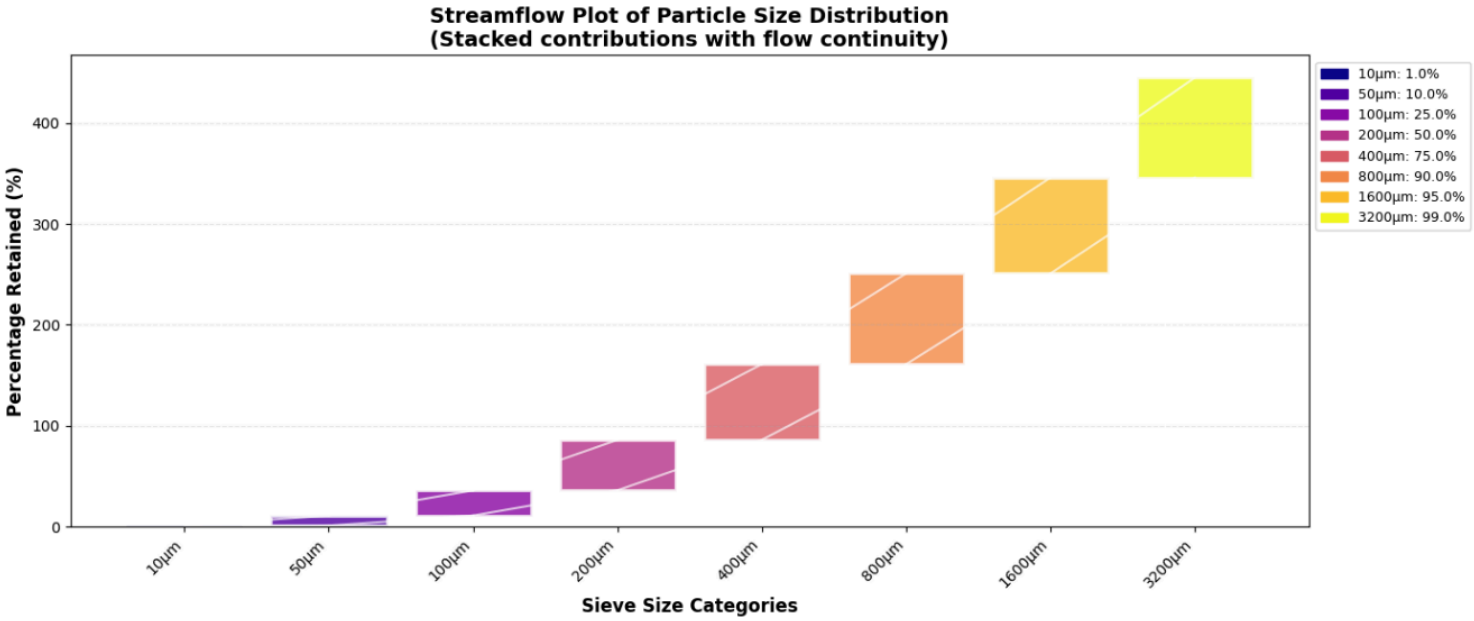


Figure 7

Stacked particle retained percentage values across different sieve size categories